Polarimetric distributed feedback fiber laser sensor for simultaneous strain and temperature measurements

O. Hadeler E. Rønnekleiv M. Ibsen

and R. I. Laming

O. Hadeler, M. Ibsen and R. I. Laming are with the Optoelectronics Research Centre, University of Southampton, Southampton SO17 1BJ, UK. E. Rønnekleiv was on leave from Optoplan AS, Box 1963, 7002 Trondheim, Norway and the Norwegian Univ. of Science and Technology, Dept. of Phys. El., 7034 Trondheim, Norway.

December 20, 1998

Abstract

We report the application of a dual polarisation distributed feedback fiber laser as a strain and temperature sensor. By measuring the absolute wavelength of one polarisation as well as the polarisation beat frequency strain and temperature were determined simultaneously. The sensor has an accuracy of $\pm 3\,\mu\epsilon$ and ± 0.04°C. Self heating of the DFB fiber laser as a function of pump power was measured with this sensor.

Key words: fiber optic sensors, fiber lasers, strain sensing, temperature sensing.

1 Introduction

Fiber optic Bragg grating sensors are a promising device for measuring strain and temperature in a variety of structures. Bragg gratings are written noninvasively into optical fibers [1, 2], making the sensor head very compact. The measurands are wavelength encoded, offering high accuracy and wavelength division multiplexing capabilities of several sensors. However, as the grating wavelength is a function of strain and temperature the elimination or compensation of this strain-temperature cross-sensitivity has become of great technological interest in recent years.

Several techniques have been developed and demonstrated to separate the strain and temperature response of fiber Bragg grating sensors. These include compensating temperature drifts by employing two independent sensors [3], one subject to strain and temperature and the second one subject to temperature only. Careful packaging and positioning of the sensors is required to ensure that the temperature difference between the two sensors remains constant and that the second sensor does not experience any strain. A more compact design can be achieved by using a single Bragg grating sensor capable of measuring strain and temperature simultaneously. By superimposing two gratings at different wavelength such a sensor has been demonstrated [4], making use of the different strain and temperature responses at the two grating wavelengths. The measurement errors were $\pm 10\,\mu\epsilon$ and ± 5°C. While such a sensor needs two light sources at widely separated wavelengths, Sudo et al. [5] have reported a sensor utilising a Bragg grating written into birefringent fiber where the grating wavelengths of the two orthogonal polarisations responded differently to strain and temperature. The maximum measurement errors of

that polarimetric sensor were $\pm 20\,\mu\epsilon$ and $\pm 2°C$. Alternatively the thermal response of a grating strain sensor can be cancelled by using a chirped grating in a tapered fiber [6]. However, the elimination of the temperature response might limit the practicality of this strain sensor for structural monitoring since it is impossible to discriminate between mechanically and thermally induced expansion.

A common disadvantage of the above mentioned passive fiber Bragg grating sensors is that only a small fraction of the spectrally broad band light incident on a narrow band grating is reflected. This limits the signal-to-noise ratio and therefore the resolution of the sensor. In general, active fiber grating sensors, i.e. sensors where gratings form part of a fiber laser, offer a higher accuracy than passive Bragg grating sensors. The laser intensity is concentrated in a spectral band which is several orders of magnitude narrower than the bandwidth of a passive grating. The laser cavities of distributed Bragg reflection (DBR) fiber lasers are formed by either a broad band mirror and a grating or two gratings at the same wavelength. Typical DBR fiber lasers are between a few centimetres and several metres long. Melle et al. [7] reported a DBR fiber laser strain sensor with a resolution of $\pm 5.4\,\mu\epsilon$, limited by electrical noise of the interrogation system. However, in this case the sensor resolution potentially suffers from mode hopping of these highly multimoded lasers caused by nonuniform environmental changes along the cavity length [7, 8]. Multiplexing of up to three DBR fiber laser sensors was demonstrated with negligible cross-talk between the sensors [9].

A DBR fiber laser may operate in orthogonal polarisation modes if birefringent fiber or birefringent gratings are used in the laser cavity. For lasers with a sufficiently small birefringence the beat frequency between the two polarisation modes can be measured

with a commercial RF spectrum analyser. External perturbations such as strain and temperature change the birefringence [10] and therefore the polarisation beat frequency. Kim et al. [11] have demonstrated a polarimetric fiber laser sensor for measuring either strain or temperature. Because of its multimode operation the RF spectrum exhibited a number of beat frequencies between different longitudinal and polarisation modes. The accuracy of the sensor was limited by the broad linewidth of the polarisation beat signal ($\sim 1.2\,\mathrm{MHz}$). A DBR fiber laser which was lasing only in two orthogonal polarisation modes was demonstrated by Ball et al. [12]. The linewidth of the polarisation beat signal was less than 2.5 kHz. Compared to multimode lasers, signal processing becomes much simpler as only one polarisation beat frequency is present. Also, the narrow linewidth of the polarisation beat signal leads to a higher measurement resolution.

For single mode operation DBR fiber lasers must not be longer than a few centimetres and the grating bandwidth has to be below $\sim 0.2\,\mathrm{nm}$. The short length usually limits the pump absorption and therefore the output power. Distributed feedback (DFB) fiber lasers are an alternative to DBR fiber lasers with the advantage that they consist of only one grating written into rare earth doped fiber. They offer single mode operation without mode hopping and kHz linewidth [13]. With a grating length of $\sim 50\,\mathrm{mm}$ DFB fiber lasers are very compact. Furthermore, as most of the laser intensity is concentrated in the centre of the grating, the sensitive region is only $\sim 5-10\,\mathrm{mm}$ long [14], making it ideal for "point" sensing. Multiplexing of five DFB fiber lasers has been demonstrated [15], but only little investigations into lasing stability and sensor accuracy have been carried out. In low birefringent fiber a DFB fiber laser can operate on two orthogonal polarisation modes with a frequency separation between the two modes sufficiently small so that the

polarisation beat signal can be measured very accurately with a commercial RF spectrum analyser. A birefringent DFB fiber laser operating stably in two polarisation modes was employed as a polarimetric sensor for separately measuring lateral forces and temperature [16].

In this article we demonstrate a similar polarimetric DFB fiber laser sensor for strain and temperature measurements. By measuring both the polarisation beat frequency and the absolute wavelength of one polarisation both measurands were determined simultaneously.

2 Theory

The wavelengths of the two orthogonal polarisation modes of a DFB fiber laser are given by

$$\lambda_{x,y} = 2n_{x,y}\Lambda, \tag{1}$$

where $\lambda_{x,y}$ denotes the wavelength of the two orthogonally polarised laser modes, $n_{x,y}$ are the refractive indices of the fiber and Λ is the grating pitch. For a low birefringent fiber with $n_x \approx n_y \approx n$ the polarisation beat frequency becomes

$$\Delta\nu = cB/(2n^2\Lambda), \tag{2}$$

where $B = n_x - n_y$ is the birefringence and c is the velocity of light. Generally the strain and temperature dependence of $\lambda_{x,y}$ is given by

$$\delta\lambda_{x,y}/\lambda_{x,y} = (1 + p_e)\delta\epsilon\Big|_{T=\text{const}} + (\alpha + \xi)\delta T\Big|_{\epsilon=\text{const}}, \tag{3}$$

where p_e is the strain-optic coefficient, α is the linear thermal expansion coefficient and ξ is the thermo-optic coefficient. Typical values for silica fiber quoted in the literature are

$p_e = -0.22$, $n_x = 1.46$, $\alpha \approx 0.5 \times 10^{-6}\,\mathrm{K}^{-1}$ and $\xi \approx 8.5 \times 10^{-6}\,\mathrm{K}^{-1}$ [16, 17].

Asymmetrical transverse stress introduces birefringence in the fiber. This stress can build up in non-circular symmetric fibers during fabrication due to the different thermal contraction of core and cladding. For temperatures below $\sim 350°\mathrm{C}$ the birefringence reduces linearly with increasing temperature as the glass softens [10]. Theoretical and experimental work [18] has shown that the birefringence is also strain dependent. Both, [10] and [18], have shown that the strain and temperature dependence of the birefringence is caused by a complex interplay between fiber asymmetries and the different mechanical and thermal properties of the core and cladding. However, the theory proposed [18] is not detailed enough to describe exactly the strain dependence of the birefringence in fibers where core and cladding have different mechanical properties. Leaving the exact birefringence mechanisms aside, it follows from Eq. (2) that $\Delta\nu$ of a birefringent DFB fiber laser changes with strain and temperature according to

$$\frac{\delta(\Delta\nu)}{\Delta\nu} = \left[\frac{1}{B}\frac{dB}{d\epsilon} - (1+2p_e)\right]\delta\epsilon\Big|_{T=\text{const}} + \left[\frac{1}{B}\frac{dB}{dT} - (\alpha+2\xi)\right]\delta T\Big|_{\epsilon=\text{const}}. \qquad (4)$$

The responses $\delta\lambda_{x,y}$ and $\delta(\Delta\nu)$ of the DFB fiber laser to strain and temperature (Eqs. 3 and 4) can be written in matrix form as

$$\begin{aligned}\begin{pmatrix}\delta\lambda_{x,y}\\ \delta(\Delta\nu)\end{pmatrix} &= \begin{pmatrix}k_{11} & k_{12}\\ k_{21} & k_{22}\end{pmatrix}\begin{pmatrix}\delta\epsilon\\ \delta T\end{pmatrix} \\ &= \boldsymbol{K}\begin{pmatrix}\delta\epsilon\\ \delta T\end{pmatrix}.\end{aligned} \qquad (5)$$

For a well conditioned matrix $\boldsymbol{K}$, i.e. $\det\boldsymbol{K} \neq 0$, Eq. (5) can be inverted. Strain and temperature can then be determined simultaneously by measuring either $\delta\lambda_x$ or $\delta\lambda_y$ and $\delta(\Delta\nu)$.

3 Experimental arrangement

The experimental arrangement is shown in Fig. 1. A 45 mm long DFB fiber laser was written in an uncoated fiber consisting of an Er^{3+}:Yb^{3+}-doped silica core, a B-Ge-doped silica photosensitive ring around the core and a silica cladding. The grating coupling coefficient was $\kappa \approx 230\,\mathrm{m}^{-1}$ and the grating phase-shift was positioned asymmetrically 20 mm away from the pump input end. The laser operated around $\lambda = 1550$ nm. Standard telecommunication fiber was spliced to both sides of the laser, approximately 5 mm away from the grating ends. The gauge length of the strain sensor was defined by bonding the coated telecommunication fiber to a fixed metal post and a manual translation stage with cyanoacrylate. Each bonded region was 10–15 mm long. The gauge length was $l_g = 616$ mm. An oven, consisting of a 150 mm × 15 mm × 15 mm aluminium block and a Peltier element, was used to heat the DFB fiber laser. A duct (3 mm × 3 mm) along the longitudinal axis of the aluminium block accommodated the DFB fiber laser. Care was taken so that the laser did not touch the aluminium block preventing unwanted strain caused by friction. Furthermore, twist in the fiber was avoided in order not to introduce additional birefringence. The temperature of the aluminium block was regulated with a commercial temperature controller. The thermistor of the control loop was placed ≈ 10 mm away from the edge of the Peltier element. The real temperature of the aluminium block was measured with a thermocouple next to the thermistor. The thermocouple had a resolution of ±0.1°C and the temperature controller kept the temperature of the oven to within this resolution. The oven was isolated by 5–15 mm thick polystyrene. The free thermal expansion of the fiber was constrained by the two fixing points of the fiber.

Therefore temperature changes of the fiber section in the oven induced thermal stress along the whole length of fiber. The stress related strain was $l_h \alpha \, \delta T / l_g$, where l_h is the length of the fiber section in the oven.

The DFB fiber laser was pumped by a 1480 nm diode laser and gave an output power of 430 μW for 82 mW of pump power. The output of the DFB fiber laser was split into two arms by a 50:50 coupler. One arm was used to measure the wavelength $\lambda_{x,y}$ of one polarisation with a wavemeter. The polarisation controller PC1 was used to align the polarisation axes of the laser output parallel to the axes of a fiber pigtailed polarising beamsplitter (PBS) so that only the x-polarisation (labelling of the polarisation axes is arbitrarily) was incident on the wavemeter. The alignment of the polarisation axes was monitored at the second output of the PBS with a scanning Fabry-Perot spectrum analyser with a free spectral range of 6 GHz and a resolution of 1.2 MHz. The polarisation controller PC1 was adjusted until the signal from the x-polarisation vanished on the Fabry-Perot trace. Measuring $\delta\lambda_{x,y}$ of only one polarisation leads to a greater accuracy than measuring the change of the mean wavelength of both polarisations. The latter method could suffer from relative intensity fluctuations between the two polarisation modes. As external perturbations of the lead fibre will change the polarisation state at the input of the PBS, active polarisation control or the use of polarisation maintaining fiber should be considered. At the other output of the coupler, the two polarisation modes were mixed in a polariser. The resulting beat signal was detected with a photodiode and the frequency measured with an RF spectrum analyser. A polarisation controller (PC2) was used to optimise the signal amplitude on the RF spectrum analyser.

4 Results

The wavelength λ_x of the unstrained DFB fiber laser at room temperature was measured to be 1549.5 nm whilst the polarisation beat frequency was $\Delta\nu \approx 1$ GHz with a linewidth of ≈ 10 kHz. Inserting $\Delta\nu$, $\lambda_x \approx 2n\Lambda$ and $n = 1.46$ into Eq. (2) leads to a birefringence of $B \approx 7.5 \times 10^{-6}$. This birefringence is a combination of the intrinsic fiber birefringence and the birefringence induced by the inscription of the DFB grating. The polarisation beat frequency of our DFB fiber laser is about 2.3 times bigger than in a previous experiment [16]. This can be attributed to the different fibers used for the two lasers as the grating writing process was essentially the same.

The sensor was calibrated by measuring λ_x and $\Delta\nu$ at four different temperatures with nine strain levels each. The standard deviation of each measurement was estimated to be $\sigma(\lambda_x) \approx \pm 1$ pm and $\sigma(\Delta\nu) \approx \pm 10$ kHz respectively. The results are shown in Figs. 2 and 3. Two planes, $\lambda_x(\epsilon, T)$ and $\Delta\nu(\epsilon, T)$, were fitted to the data yielding the following regression coefficients and their standard deviation:

$$
\begin{aligned}
k_{11} &= (1.147 \pm 0.002)\,\mathrm{pm}/\mu\epsilon, \\
k_{12} &= (7.946 \pm 0.065)\,\mathrm{pm}/^{\circ}\mathrm{C}, \\
k_{21} &= (7.946 \pm 0.043)\,\mathrm{kHz}/\mu\epsilon, \\
k_{22} &= (-1.623 \pm 0.002)\,\mathrm{MHz}/^{\circ}\mathrm{C}.
\end{aligned}
$$

Note that the numerical equality of k_{12} and k_{21} is a pure coincidence.

The analysis of the residuals showed that the deviations of the wavelength measurements from the fitted straight line mainly arose from an uneven motion of the translation stage which defined the strain. This limits the accuracy of the regression coefficients k_{11} and

k_{12}. The resolution ($\pm 0.1\,°C$) of the thermocouple used to measure the oven temperature corresponds to $\delta(\Delta\nu) = \pm 162\,\mathrm{kHz}$. The residuals of the beat frequency measurements and the resulting standard deviation of the regression coefficients k_{21} and k_{22} are mainly due to this limited resolution of the temperature measurement. The analysis of the residuals showed no sign of nonlinear strain or temperature response of the sensor. Therefore it can be concluded that any cross-sensitivity between strain and temperature is negligible. By combining the calibration errors, i.e. the errors of $\boldsymbol{K}^{-1}$, and the accuracies of the wavelength and polarisation beat frequency measurements, $\sigma(\lambda_x)$ and $\sigma(\Delta\nu)$, the accuracy of this strain and temperature sensor is $\pm 3\,\mu\epsilon$ and $\pm 0.04°C$. The reproducibility of the strain measurements was $\pm 2.5\,\mu\epsilon$ which is in agreement with the position reproducibility of the translation stage. Although the telecommunication fiber was coated no slipping or creep of the fiber was observed. However, at higher strain levels or over longer periods of time slipping and creep are potential problems which can be solved by choosing appropriate glues and using either uncoated fiber or harder coatings. The thermal stress induced by the rise of the fiber temperature from room temperature (25°C) to 45°C lead to a strain of $\approx 2.4\,\mu\epsilon$, which lies within the accuracy of the sensor. A possible calibration error of the thermometer is not included in the above stated accuracy of the sensor. The resolution of this strain and temperature sensor is limited by the accuracy of the wavelength and beat frequency measurements. The accuracy of the wavelength measurement is practically limited by the wavemeter used, in this case $\pm 0.1\,\mathrm{pm}$. The accuracy of the beat frequency measurement is limited by the linewidth of the beat signal, which in turn depends on the linewidth of the DFB fiber laser.

The strain dependence $\delta\lambda_x/\lambda_x = k_{11} \times \delta\epsilon/\lambda_x = 0.74\delta\epsilon$ is in good agreement with the-

oretical predictions from Eq. (3) of $\delta\lambda_x/\lambda_x = 0.78\delta\epsilon$. The temperature dependence $\delta\lambda_x/\lambda_x = k_{12} \times \delta T/\lambda = 5.1 \times 10^{-6}\,\mathrm{K}^{-1}$ is smaller than $8.5 \times 10^{-6}\,\mathrm{K}^{-1}$, the value commonly quoted for silica fiber in the literature. This discrepancy probably arises from the rare earth doping of the fiber as the value is similar to $4.9 \times 10^{-6}\,\mathrm{K}^{-1}$ calculated from the results published in [16]. From the beat frequency measurement $\Delta\nu$ it can be concluded that the birefringence increases with strain. Additional asymmetric stress is probably induced in the strained fiber due to different mechanical properties of the core, the B-Ge-doped ring and the cladding. The decrease of $\Delta\nu$ with increasing temperature is expected from theory. The slope $\delta(\Delta\nu)/\delta T$ depends on the actual thermal properties of the fiber used. Self heating of the DFB fiber laser sensor, which is a function of pump power, is a potential source of error. Since the laser intensity is concentrated in the centre of the grating and decreases exponentially towards the ends [14] the temperature varies accordingly. Measuring λ_x and $\Delta\nu$ yields a weighted mean or effective temperature of the DFB fiber laser. While the unstrained fiber was in free air in the oven the pump power was increased from 40 mW to 85 mW. Fig. 4 shows λ_x and $\Delta\nu$ as a function of pump power. The data points lie within the aforementioned accuracy. Fitting two straight lines to the data and using the calibration constants k_{12} and k_{22} reveals that the effective temperature increased by (0.014 ± 0.001)°C/mW. In order not to exceed the aforementioned accuracy of ± 0.04°C the pump power must not vary by more than ± 3 mW. While the output power of commercial pump lasers can easily be stabilised to within this limit, variable losses in the lead fiber could potentially cause larger variations. Further investigations on how the pump and lasing intensities heat the fiber will be carried out in a separate experiment.

5 Conclusion

In conclusion, we have demonstrated an active polarimetric strain and temperature sensor based on a birefringent DFB fiber laser. The achieved accuracy of simultaneous measurements of strain and temperature was $\pm 3\,\mu\epsilon$ and $\pm 0.04°C$ respectively. This accuracy was limited by the equipment used to calibrate the sensor so an improved accuracy should be obtainable. No cross-sensitivity between strain and temperature was observed, the sensor responded linearly to both measurands. The DFB fiber laser operated robustly in two linear polarisations and it is hoped that multiplexing of several such devices will lead to simple, easy to install and reliable fiber sensor networks. For industrial applications the sensor can potentially be protected by e.g. tubes of $\sim 50\,\text{mm}$ length and $\sim 1\,\text{mm}$ diameter. Mass fabrication of DFB fiber lasers would result in a low cost sensor head. The expensive parts of the sensor, the pump laser and signal processing unit, could be shared between several sensor networks. The use of a digital frequency counter or a voltage controlled oscillator locked to the polarisation beat frequency would reduce the costs of the signal processing unit. Self heating of the fiber laser as a function of pump power has also been measured. Pump power fluctuations which could be caused by variable losses in the lead fiber should be kept below $\pm 3\,\text{mW}$ in order not to exceed the previously mentioned accuracy of the temperature measurements.

O. Hadeler acknowledges support through a CASE award from BICC and the useful discussions with the staff at BICC in Helsby, UK. The Optoelectronics Research Centre is

an interdisciplinary research centre funded by the UK Engineering and Physical Science Research Council.

References

[1] G. Meltz, W. W. Morey, and W. H. Glenn, "Formation of Bragg gratings in optical fibers by a transverse holographic method," Opt. Lett. **14**, 823–825 (1989)

[2] K. O. Hill, B. Malo, F. Bilodeau, D. C. Johnson, and J. Albert, "Bragg gratings fabricated in monomode photosensitive optical fiber by UV exposure through a phase mask," Appl. Phys. Lett. **62**, 1035–1037 (1993)

[3] A. D. Kersey, T. A. Berkoff, and W. W. Morey, "Fiber-optic Bragg grating strain sensor with drift-compensated high-resolution interferometric wavelength-shift detection," Opt. Lett. **18**, 72–74 (1993)

[4] M. G. Xu, J.-L. Archambault, L. Reekie, and J.P. Dakin, "Discrimination between strain and temperature effects using dual-wavelength fibre grating sensors," Electr. Lett. **30**, 1085–1087 (1994)

[5] M. Sudo, M. Nakai, K. Himeno, S. Suzaki, A. Wada, and R. Yamauchi, "Simultaneous measurement of temperature and strain using PANDA fiber grating," in *12th Int. Conf. Opt. Fiber Sens.*, Vol. 16, OSA Tech. Digest Series (Optical Society of America, Washington DC, 1997), 170–173

[6] M. G. Xu, L. Dong, L. Reekie, J. A. Tucknott, and J. L. Cruz, "Temperature-independent strain sensor using a chirped Bragg grating in a tapered optical fibre," Electr. Lett. **31**, 823–825 (1995)

[7] S. M. Melle, A. T. Alavie, S. Karr, T. Coroy, K. Liu, and R. M. Measures, "A Bragg grating-tuned fiber laser strain sensor system," IEEE Phot. Technol. Lett. **5**, 263–266 (1993)

[8] G. A. Ball, W. W. Morey, and P. K. Cheo, "Single- and multipoint fiber-laser sensors," IEEE Phot. Technol. Lett. **5**, 267–270 (1993)

[9] A. T. Alavie, S. E. Karr, A. Othonos, and R. M. Measures, "A multiplexed Bragg grating fiber laser sensor system," IEEE Phot. Technol. Lett. **5**, 1112–1114 (1993)

[10] S.C. Rashleigh, "Origins and control of polarization effects in single-mode fibers," J. Lightwave Technol. **LT-1**, 312–331 (1983)

[11] H. K. Kim, S. K. Kim, and B. Y. Kim, "Polarization control of polarimetric fiber-laser sensors," Opt. Lett. **18**, 1465–1467 (1993)

[12] G. A. Ball, G. Meltz, and W. W. Morey, "Polarimetric heterodyning Bragg-grating fiber-laser sensor," Opt. Lett. **18**, 1976–1978 (1993)

[13] J. T. Kringlebotn, J.-L. Archambault, L. Reekie, and D. N. Payne, "Er^{3+}:Yb^{3+}-codoped fiber distributed-feedback laser," Opt. Lett. **19**, 2101–2103 (1994)

[14] E. Rønnekleiv, M. Ibsen, M. N. Zervas, and R. I. Laming, "Characterization of intensity distribution in symmetric and asymmetric fiber DFB lasers," in *Conf. on Lasers and Electro-Optics*, Vol. 6, 1998 OSA Tech. Digest Series (Optical Society of America, Washington DC, 1998), 80

[15] J. Hübner, P. Varming, and M. Kristensen, "Five wavelength DFB fibre laser source for WDM systems," Electr. Lett. **33**, 139–140 (1997)

[16] J. T. Kringlebotn, W. H. Loh, and R. I. Laming, "Polarimetric Er^{3+}-doped fiber distributed-feedback laser sensor for differential pressure and force measurements," Opt. Lett. **21**, 1869–1871 (1996)

[17] H. Singh, and J. S. Sirkis, "Simultaneously measuring temperature and strain using optical fiber microcavities," J. Lightwave Technol. **15**, 647–653 (1997)

[18] S.-Y. Huang, J. N. Blake, and B. Y. Kim, "Perturbation effects on mode propagation in highly elliptical core two-mode fibers," J. Lightwave Technol. **8**, 23–33 (1990)

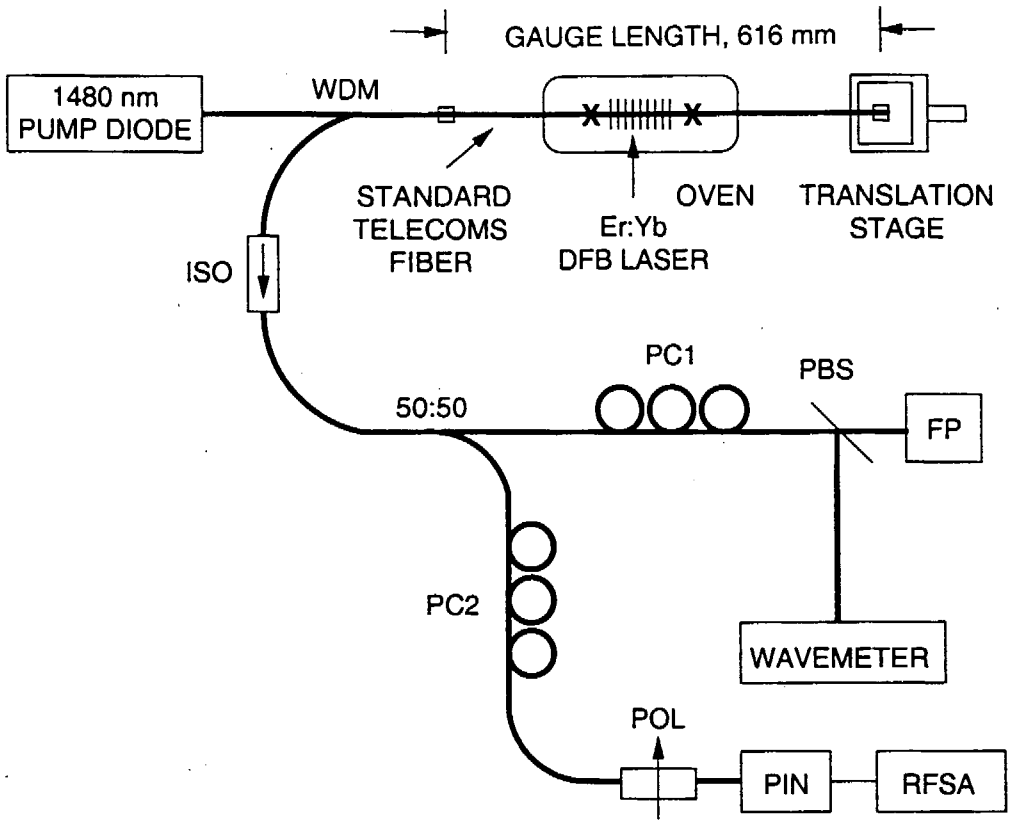
GAUGE LENGTH, 616 mm
1480 nm
PUMP DIODE
WDM
STANDARD
TELECOMS
FIBER
OVEN
Er:Yb
DFB LASER
TRANSLATION
STAGE
ISO
PC1
PBS
50:50
FP
PC2
WAVEMETER
POL
PIN
RFSA

Fig. 1

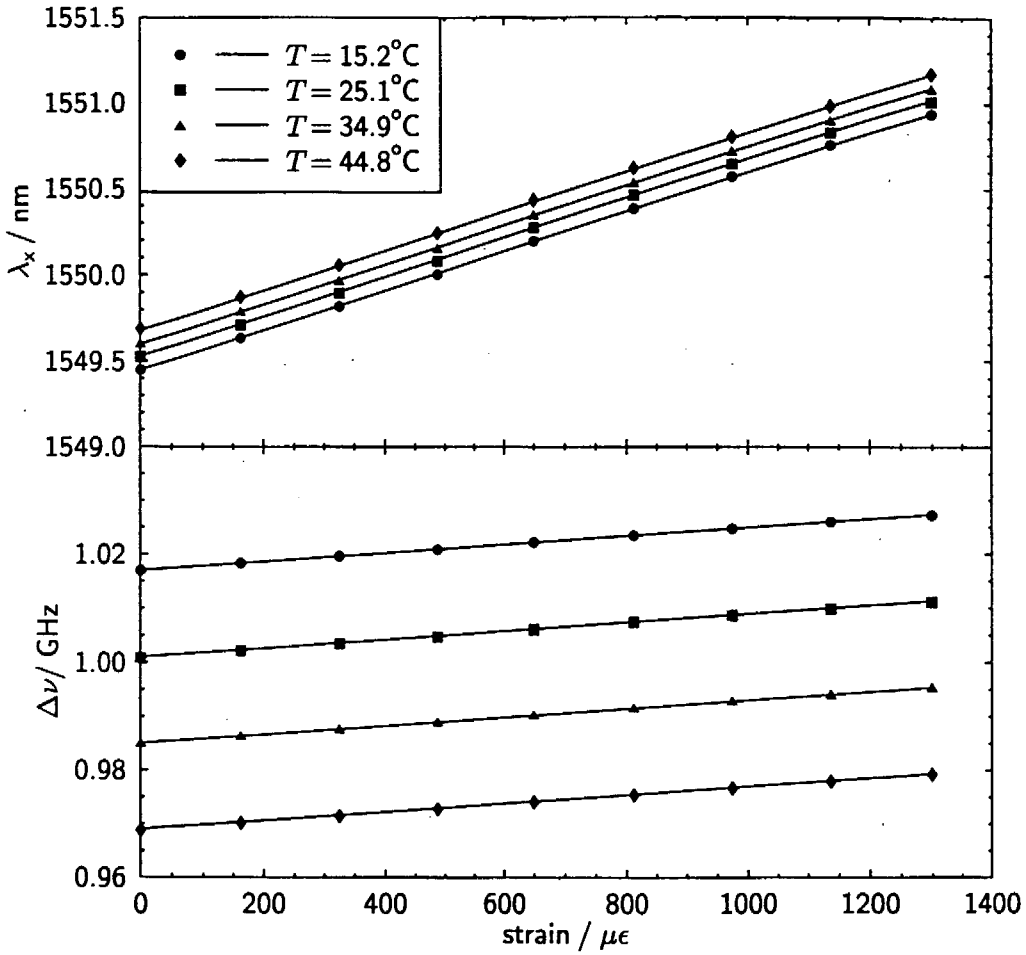
1551.5
1551.0
1550.5
1550.0
1549.5
1549.0
λ_x / nm
$T = 15.2°C$
$T = 25.1°C$
$T = 34.9°C$
$T = 44.8°C$
1.02
1.00
0.98
0.96
$\Delta\nu$/ GHz
0
200
400
600
800
1000
1200
1400
strain / $\mu\epsilon$

Fig. 2

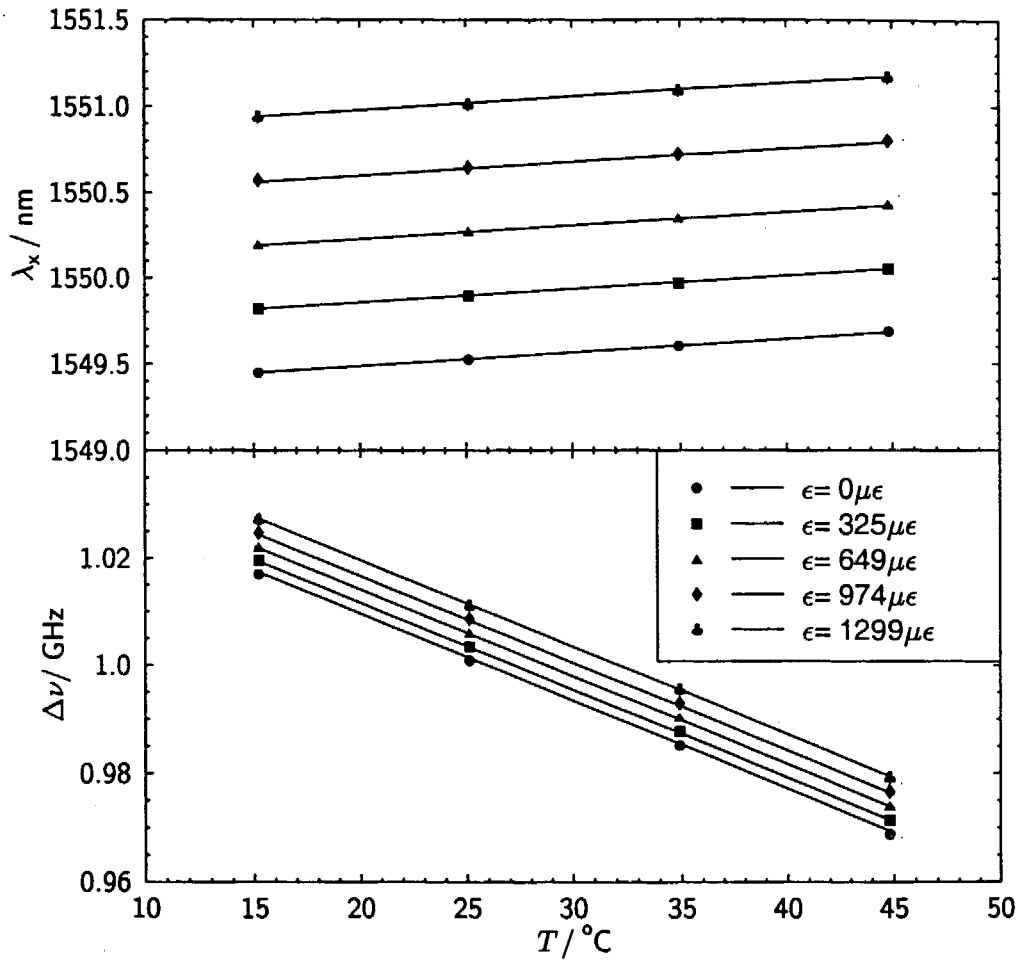
1551.5
1551.0
1550.5
1550.0
1549.5
1549.0
λ_x / nm
1.02
1.0
0.98
0.96
$\Delta\nu$ / GHz
10
15
20
25
30
35
40
45
50
T / °C
ϵ= 0$\mu\epsilon$
ϵ= 325$\mu\epsilon$
ϵ= 649$\mu\epsilon$
ϵ= 974$\mu\epsilon$
ϵ= 1299$\mu\epsilon$

Fig. 3

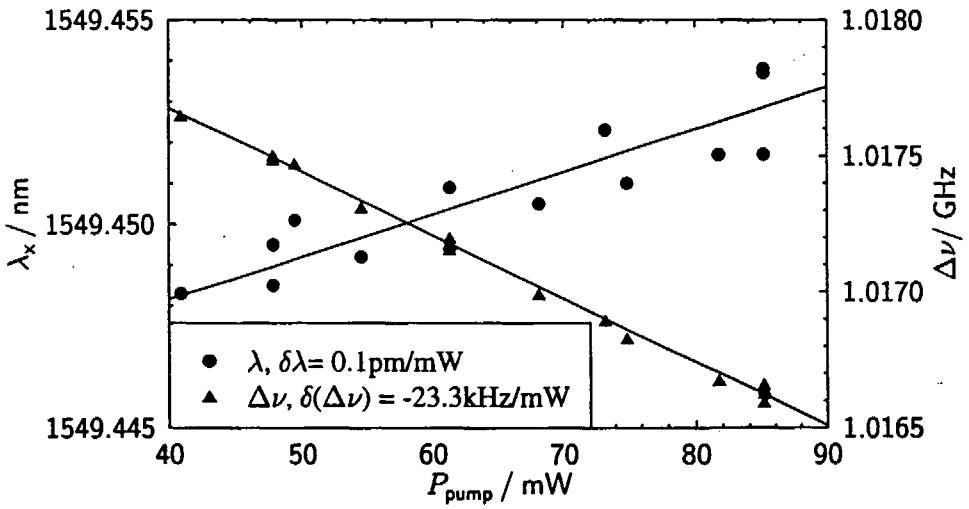
1549.455
1549.450
1549.445
1.0180
1.0175
1.0170
1.0165
40
50
60
70
80
90
λ_x / nm
$\Delta\nu$ / GHz
P_{pump} / mW
λ, $\delta\lambda$= 0.1pm/mW
$\Delta\nu$, $\delta(\Delta\nu)$ = -23.3kHz/mW

Fig. 4

Figure 1: Experimental arrangement, WDM=wavelength division multiplexer, ISO=isolator, 50:50=coupler, PC1 and PC2=polarisation controllers, PBS=polarising beam splitter, POL=polariser, FP=Fabry-Perot spectrometer, PIN=photodiode, RFSA=RF spectrum analyser.

Figure 2: Wavelength of x-polarisation and polarisation beat frequency as a function of strain.

Figure 3: Wavelength of x-polarisation and polarisation beat frequency as a function of temperature. Data of only five strain levels is shown for clarity of the graph.

Figure 4: Wavelength of x-polarisation and polarisation beat frequency as a function of pump power at 1480 nm.